

A sparse matrix formulation of model-based ensemble Kalman filter

Håkon Gryvill and Håkon Tjelmeland

Department of Mathematical Sciences, Norwegian University of Science and Technology, Alfred Getz' vei 1, Trondheim, 7034, Norway.

*Corresponding author(s). E-mail(s): hakon.gryvill@ntnu.no;
Contributing authors: haakon.tjelmeland@ntnu.no;

Abstract

We introduce a computationally efficient variant of the model-based ensemble Kalman filter (EnKF). We propose two changes to the original formulation. First, we phrase the setup in terms of precision matrices instead of covariance matrices, and introduce a new prior for the precision matrix which ensures it to be sparse. Second, we propose to split the state vector into several blocks and formulate an approximate updating procedure for each of these blocks. We study in a simulation example the computational speedup and the approximation error resulting from using the proposed approach. The speedup is substantial for high dimensional state vectors, allowing the proposed filter to be run on much larger problems than can be done with the original formulation. In the simulation example the approximation error resulting from using the introduced block updating is negligible compared to the Monte Carlo variability inherent in both the original and the proposed procedures.

Keywords: Bayesian inference, data assimilation, ensemble Kalman filter, Gaussian Markov random field, hidden Markov model, spatial statistics

1 Introduction

State-space models are frequently used in many applications. Examples of application areas are economics ([Creal, 2011](#); [Chan and Strachan, 2020](#)),

weather forecasting (Houtekamer and Zhang, 2016; Hotta and Ota, 2021), signal processing (Loeliger et al, 2007) and neuroscience (Smith and Emery, 2003). A state-space model consists of an unobserved latent $\{x_t\}$ discrete time Markov process and a related observed $\{y_t\}$ process, where y_t gives information about x_t , and the y_t 's are assumed to be conditionally independent given the $\{x_t\}$ process. Given observed values y_1, \dots, y_t the goal is to do inference about one or more of the x_t 's. In this article the focus is on the filtering problem, where the goal is to find the conditional distribution of x_t given observations $y_{1:t} = (y_1, \dots, y_t)$. The filtering problem is also known as sequential data assimilation and online inference.

The Markov structure in the specification of the state-space model allows the filtering problem to be solved recursively. Having available a solution of the filtering problem at time $t - 1$, i.e. the distribution $p(x_{t-1}|y_{1:t-1})$, one can first use this filtering distribution to find the one-step forecast distribution $p(x_t|y_{1:t-1})$, which one in turn can combine with the observed data at the next time step, y_t , to find $p(x_t|y_{1:t})$. The identification of the forecast distribution is often termed the forecast or prediction step, whereas the process of finding the filtering distribution is called the update or analysis step. If a linear-Gaussian model is assumed analytical solutions are available both for the forecast and update steps, and is known as the Kalman filter (Kalman, 1960; Kalman and Bucy, 1961). Another situation where an analytical solution is available for the forecast and update steps is when x_t is a vector of categorical or discrete variables. In essentially all other situations, however, analytical solutions are not available and one has to resort to approximate solutions. Ensemble-based methods are here the most popular choice, where each distribution of interest is represented by a set of particles, or an ensemble of realisations, from the distribution of interest. In ensemble-based methods one also alternates between a forecast and an update step. The forecast step is straightforward to implement without approximations in ensemble methods, whereas the update step is challenging. In the update step an ensemble of realisations, x_t^1, \dots, x_t^M , from the forecast distribution $p(x_t|y_{1:t-1})$ is available and the task is to update each realisation x_t^m to a corresponding realisation \tilde{x}_t^m from the filtering distribution $p(x_t|y_{1:t})$. The forecast distribution $p(x_t|y_{1:t-1})$ serves as a prior in the update step, and the filtering distribution $p(x_t|y_{1:t})$ is the resulting posterior. In the following we therefore refer to the ensemble of realisations from the forecast distribution as the prior ensemble and the ensemble of realisations from the filtering distribution as the posterior ensemble.

There are two popular classes of ensemble filtering methods, particle filters (Doucet et al, 2001; Doucet and Johansen, 2011) and ensemble Kalman filters (EnKFs) (Burgers et al, 1998; Evensen, 2009). Particle filters are based on importance sampling and resampling and has the advantage that it can be shown to converge to the correct filtering solution in the limit when the number of particles goes towards infinity. However, in applications with high dimensional state vectors, x_t , particle filters typically collapse when run with a finite number of particles. The updating procedure in EnKFs is based on a

linear-Gaussian model, but experience in applications is that EnKFs produce good results also in situations where the linear-Gaussian assumptions are not fulfilled. However, except when the linear-Gaussian model is correct the EnKF is only approximate, even in the limit when the number of ensemble elements goes towards infinity. Most of the EnKF literature is in applied journals and has not much focus on the underlying statistical theory, but some publications has also appeared in statistical journals (Sætrom and Omre, 2013; Katzfuss et al, 2016, 2020; Loe and Tjelmeland, 2020, 2022).

In EnKF the update step consists of two parts. First a prior covariance matrix is established based on the prior ensemble, which thereafter is used to modify each prior ensemble element to a corresponding posterior element. Many variants of the original EnKF algorithm of Evensen (1994) have been proposed and studied in the literature, see for example Evensen (2009) and Houtekamer and Zhang (2016) and references therein. In particular the original algorithm of Evensen (1994) is known to severely underestimate the uncertainty and much attention has focused on how to correct for this. The most frequent approach to this problem is the rather ad hoc solution of variance inflation, see the discussion in Luo and Hoteit (1997). Houtekamer and Mitchell (1997) identified the source of the problem to be inbreeding, that the same prior ensemble elements that are first used to establish the prior covariance matrix are thereafter modified into posterior ensemble elements. To solve this problem Houtekamer and Mitchell (1997) proposed to split the prior ensemble in two, where the prior ensemble elements in one part is used to establish a prior covariance matrix which is used when modifying the prior ensemble elements in the other part into corresponding posterior elements. As discussed in Houtekamer and Zhang (2016) this cross validation setup is later generalised to a situation where the prior ensemble is split into more than two parts. Myrseth et al (2013) propose to use a resampling approach to solve the inbreeding problem. Another issue with the original EnKF setup of Evensen (2009) that has been focused in the literature is that the empirical covariance matrix of the prior ensemble is used as the prior covariance matrix, thereby effectively ignoring the associated estimation uncertainty. To cope with this problem Omre and Myrseth (2010) set the problem of identifying the prior covariance matrix in a Bayesian setting. A normal inverse Wishart prior is defined for the mean vector and the covariance matrix of the prior ensemble elements and the covariance matrix to be used in the updating of an ensemble element is sampled from the corresponding posterior distribution. Corresponding Bayesian schemes for establishing the prior covariance matrix are later adopted in Bocquet (2011), Bocquet et al (2015) and Tsyrlunikov and Rakitko (2017). Loe and Tjelmeland (2021) propose to base the updating step of the EnKF on an assumed Bayesian model for all variables involved. The updating step is defined by restricting it to be consistent with the assumed model at the same time as it should be robust against modelling error. Both the need for defining a prior for the covariance matrix and the cross validation approach discussed above comes as necessary consequences of this setup. In addition it

entails that the new data y_t should be taken into account when generating the prior covariance matrix.

In the present article we adopt the model-based EnKF approach of [Loe and Tjelmeland \(2021\)](#), but our focus is to formulate a computationally efficient variant of this approach. To obtain this we do two important changes. First, in [Loe and Tjelmeland \(2021\)](#) a normal inverse Wishart prior is used for the mean vector and covariance matrix of the prior ensemble elements. When sampling from the corresponding posterior distribution this results in a covariance matrix that is full. To update a prior ensemble element to the corresponding posterior element the covariance matrices must be used in a series of matrix operations, such as various matrix decompositions and multiplications with vectors. We rephrase the approach of [Loe and Tjelmeland \(2021\)](#) to use precision matrices, or inverse covariance matrices, instead of covariance matrices and propose a new prior distribution which ensures the precision matrices sampled from the resulting posterior to be band matrices. With a band structure in the precision matrix some of the matrix operations in the updating of a prior ensemble element to the corresponding posterior element can be done more efficiently. However, some of the matrix operations, singular value decompositions, do not benefit from this band structure. To make also this part of the procedure computationally more efficient we propose to do an approximation which allows us to replace the singular value decomposition of one large matrix with singular value decompositions of several smaller matrices.

This article is structured as follows. In [Section 2](#) we first review some numerical algorithms for sparse matrices and some properties of the Gaussian density. In the same section we also present the state-space model. In [Section 3](#) we rephrase the approach introduced in [Loe and Tjelmeland \(2021\)](#) to use precision matrices instead of covariance matrices. The new prior for the precision matrix is proposed in [Section 4](#). In [Section 5](#) we propose a computationally efficient approximation of the updating procedure presented in [Section 3](#). We present results of a simulation example in [Section 6](#), and finally we provide some closing remarks in [Section 7](#).

2 Preliminaries

This section introduces material necessary to understand the approach proposed in later sections. We start by discussing some numerical properties of sparse matrices, thereafter review how the multivariate Gaussian distribution can be formulated in terms of precision matrices. Lastly, we introduce the state-space model and provide a brief introduction on simulation-based techniques.

2.1 Numerical properties of sparse matrices

Suppose that $x, y \in \mathbb{R}^n$, that $Q \in \mathbb{R}^{n \times n}$ is a given symmetric positive definite band matrix with bandwidth p , where $n \gg p$, that y is given, and that we

want to solve the matrix equation

$$Qx = y \quad (1)$$

with respect to x . Since we assume that Q is a symmetric matrix, we can solve the equation above using the Cholesky decomposition $Q = LL^T$, where $L \in \mathbb{R}^{n \times n}$ is a lower triangular matrix. Due to the band structure of Q we know that L has lower bandwidth p , which in turn enables us to compute L with complexity $\mathcal{O}(np^2)$, see Algorithm 2.9 in [Rue and Held \(2005\)](#). Since we now are able to compute L efficiently, we can make use of Algorithm 2.1 in [Rue and Held \(2005\)](#) to solve (1) efficiently as well. In the following, we describe the algorithm step by step.

First, we rewrite (1) as

$$LL^T x = y. \quad (2)$$

If we define $L^T x = v$, we can solve (1) by first solving $Lv = y$ for v and then solving $L^T x = v$ for x . We can exploit the band structure of L to solve these equations efficiently. Using that L is lower triangular, we can solve $Lv = y$ row by row, using "forward substitution" ([Rue and Held, 2005](#), p. 32). We denote the (i, j) th entry of L as $L^{i,j}$ and the i th element of y as y^i . The i th element of v , denoted v^i , is computed as follows

$$v^i = \frac{1}{L^{i,i}} (y^i - \sum_{j=\max\{0, i-p\}}^{i-1} L^{i,j} v^j). \quad (3)$$

Similarly, we can solve $v = L^T x$ for x using "backward substitution"

$$x^i = \frac{1}{L^{i,i}} (v^i - \sum_{j=i+1}^{\min\{i+p, n\}} L^{j,i} x^j). \quad (4)$$

Notice that we compute the entries of x "backwards"; we first compute x^n and then move our way backwards to x^1 . If we again assume $n \gg p$, the computational complexity of forward and backward substitution is $\mathcal{O}(np)$. This means that the overall complexity of computing x using the presented approach is $\mathcal{O}(np^2)$. Note that solving (1) with the "brute force" approach, i.e. computing $x = Q^{-1}y$, has computational complexity $\mathcal{O}(n^3)$.

Backward substitution can also be used to sample efficiently from a Gaussian distribution when the precision matrix is a band matrix. Assume that z is a vector of standard normally distributed variables and that we want to simulate x from a Gaussian distribution with mean 0 and covariance matrix Q^{-1} . We can simulate x by solving

$$L^T x = z \quad (5)$$

using backward substitution, as specified in (4). When Q is a band matrix with bandwidth p , where $n \gg p$, the computational complexity is $\mathcal{O}(np^2)$. However, when Q is full the computational complexity of simulating x is $\mathcal{O}(n^3)$.

2.2 Gaussian distribution phrased with precision matrices

Let $x \in \mathbb{R}^n$ have a multivariate Gaussian distribution with mean $\mu \in \mathbb{R}^n$ and precision matrix $Q \in \mathbb{R}^{n \times n}$. We let $\mathcal{N}(x; \mu, Q)$ denote the density function of this distribution, i.e.

$$\mathcal{N}(x; \mu, Q) = (2\pi)^{-n/2} |Q|^{1/2} \exp\left(-\frac{1}{2}(x - \mu)^T Q (x - \mu)\right). \quad (6)$$

Defining $A \subset \{1, \dots, n\}$ and $B = \{1, \dots, n\} \setminus A$, we can partition x , μ and Q into blocks

$$x = \begin{pmatrix} x^A \\ x^B \end{pmatrix}, \quad \mu = \begin{pmatrix} \mu^A \\ \mu^B \end{pmatrix}, \quad Q = \begin{pmatrix} Q^{AA} & Q^{AB} \\ Q^{BA} & Q^{BB} \end{pmatrix}. \quad (7)$$

According to Theorem 2.5 in [Rue and Held \(2005\)](#), we then have that

$$p(x^A | x^B) = \mathcal{N}(x^A; \mu^A - (Q^{AA})^{-1} Q^{AB} (x^B - \mu^B), Q^{AA}). \quad (8)$$

Similarly,

$$p(x^B) = \mathcal{N}(x^B; \mu^B, Q^{BB} - (Q^{AB})^T (Q^{AA})^{-1} Q^{AB}). \quad (9)$$

The last expression can be derived by picking out the parts of the mean vector μ and covariance matrix Q^{-1} that corresponds to x^B . When we have found the covariance matrix of x^B we find the precision matrix by inversion. From the first expression we see that computing the precision matrix for $x^A | x^B$ is particularly easy when the Gaussian distribution is formulated with precision matrices.

2.3 State-space model

A state-space model ([Shumway and Stoffer, 2016](#); [Brockwell and Davis, 1990](#)) consists of a set of latent variables, denoted $\{x_t\}_{t=1}^T$, $x_t \in \mathbb{R}^{n_x}$, and a set of observations $\{y_t\}_{t=1}^T$, $y_t \in \mathbb{R}^{n_y}$. The latent variables follow a first order Markov chain with initial distribution $p(x_1)$ and transition probabilities $p(x_t | x_{t-1})$, $t \geq 2$. That is, the joint distribution for $x_{1:T} = (x_1, \dots, x_T)$ can be written as

$$p(x_{1:T}) = p(x_1) \prod_{t=2}^T p(x_t | x_{t-1}). \quad (10)$$

In addition, each observation y_t is considered to be conditionally independent of the remaining observations, given x_t . The joint likelihood for the observations $y_{1:T} = (y_1, \dots, y_T)$ can be formulated as

$$p(y_{1:T} | x_{1:T}) = \prod_{t=1}^T p(y_t | x_t). \quad (11)$$

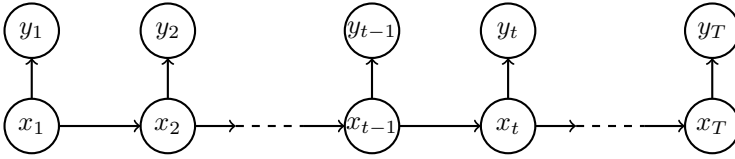


Fig. 1 DAG illustration of a state space model. The edges illustrate the stochastic dependencies between the nodes. The latent variables $x_t, t = 1, \dots, T$ are unobserved, while $y_t, t = 1, \dots, T$ are observations

A state-space model is illustrated by a directed acyclic graph (DAG) in Figure 1, where each variable is represented with a node and the edges symbolise the dependencies between the variables.

The main interest of this article, and the reason we introduce the state-space model, is to assess the filtering problem. The objective of the filtering problem is to compute the filtering distribution, $p(x_t|y_{1:t})$, for $t = 1, \dots, T$. That is, we want to find the distribution for the latent variable at time t , i.e. x_t , given all of the observations up to the same time step, $y_{1:t}$. Due to the Markov assumptions made in the state-space model, we are in principle able to assess this quantity sequentially. Each iteration is performed in two steps, namely

$$p(x_t|y_{1:t-1}) = \int p(x_t|x_{t-1})p(x_{t-1}|y_{1:t-1})dx_{t-1}, \quad (12)$$

$$p(x_t|y_{1:t}) = \frac{p(x_t|y_{1:t-1})p(y_t|x_t)}{\int p(x_t|y_{1:t-1})p(y_t|x_t)dx_t}. \quad (13)$$

The first expression is the prediction step and gives the forecast distribution $p(x_t|y_{1:t-1})$, while the second expression is called the update step and yields the filtering distribution $p(x_t|y_{1:t})$. Note that the filtering distribution is computed through Bayes' rule, where $p(x_t|y_{1:t-1})$ is the prior, $p(y_t|x_t)$ is the likelihood and $p(x_t|y_{1:t})$ is the posterior. In the following we therefore use the terms prior and forecast, and the terms posterior and filtering, interchangeably. In this article, our main focus is on the update step.

When the state-space model is linear and Gaussian, the expressions can be solved analytically through the Kalman filter (Kalman, 1960). However, the prediction and update steps in (12) and (13) are generally speaking not feasible to solve analytically. Hence approximative methods are used. A common approach is to use simulation-based techniques, where a set of realisations, which is called an ensemble, are used to explore the state-space model by moving the realisations forward in time according to the state-space model. The filtering and forecast distributions are then represented by an ensemble at each time step, which is initially sampled from $p(x_1)$. The following paragraph provides an overview of how this is done for one iteration.

Assume that a set of \mathcal{M} independent realisations $\{\tilde{x}_{t-1}^1, \dots, \tilde{x}_{t-1}^{\mathcal{M}}\}$ from $p(x_{t-1}|y_{1:t-1})$ is available at time t . If we are able to simulate from the forward model $p(x_t|x_{t-1})$, we can obtain \mathcal{M} independent realisations from $p(x_t|y_{1:t-1})$ by simulating from $x_t^{(m)}|\tilde{x}_{t-1}^{(m)} \sim p(x_t|\tilde{x}_{t-1}^{(m)})$ independently for $m = 1, \dots, \mathcal{M}$.

This is the prediction step, and can usually be performed without any approximations. Next, we use the prediction, or prior, ensemble $\{x_{t-1}^1, \dots, x_{t-1}^M\}$ to obtain samples from the filtering distribution $p(x_t|y_{1:t})$, which is often called a posterior ensemble. This can be done by conditioning the samples from the forecast distribution, $\{x_t^{(1)}, \dots, x_t^{(M)}\}$, on the new observation y_t . This step is called the update step and is generally not analytically feasible. Hence approximate methods are necessary. In the following section, we present a procedure that enables us to carry out the update step.

3 Model-based EnKF

In this section we start by reviewing the model-based EnKF framework introduced in [Loe and Tjelmeland \(2021\)](#). The focus in our presentation is on the underlying model framework, the criterion used for selecting the particular chosen update, and on the resulting updating procedure. We do not include the mathematical derivations leading to the computational procedure. Moreover, we phrase the framework in terms of precision matrices, whereas [Loe and Tjelmeland \(2021\)](#) use covariance matrices.

The focus in the section is on how to use a prior ensemble $\{x_t^{(1)}, \dots, x_t^{(M)}\}$ to update one of these prior ensemble elements, number m say, to a corresponding posterior ensemble element $\tilde{x}_t^{(m)}$. All the variables involved in this operation are associated with the same time t . To simplify the notation we therefore omit the time subscript t in the following discussion. So we write $\{x^{(1)}, \dots, x^{(M)}\}$ instead of $\{x_t^{(1)}, \dots, x_t^{(M)}\}$ for the available prior ensemble, we write $\tilde{x}^{(m)}$ instead of $\tilde{x}_t^{(m)}$ for the generated posterior ensemble element number m , we write x instead of x_t for the latent variable at time t , and we write y instead of y_t for the new data that becomes available at time t .

3.1 Assumed Bayesian model

In model-based EnKF the updating of a prior ensemble element $x^{(m)}$ to the corresponding posterior ensemble element $\tilde{x}^{(m)}$ is based on an assumed model. The dependence structure of the assumed model is illustrated in the DAG in [Figure 2](#). It should be noted that the assumed model is not supposed to be correct, it is just used as a mean to formulate a reasonable and consistent updating procedure. To stress this we follow the notation in [Loe and Tjelmeland \(2021\)](#) and use f as the generic symbol for all densities associated to the assumed model, whereas we continue to use p to denote the corresponding correct (and typically unknown) densities. We use subscripts on f to specify what stochastic variables the density relates to. For example $f_{y|x}(y|x)$ is the conditional density for the new observations y given the latent variable x .

In the assumed model we let the prior ensemble elements $x^{(1)}, \dots, x^{(M)}$ and the unobserved latent variable x at time t be conditionally independent and identically Gaussian distributed with a mean vector μ and a precision

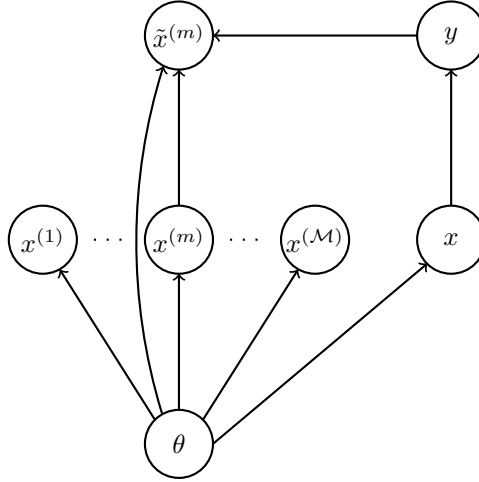


Fig. 2 DAG representation of the assumed Bayesian model for updating the m th realisation matrix Q , i.e.

$$f_{x|\theta}(x|\theta) = \mathcal{N}(x; \mu, Q), \quad (14)$$

$$f_{x^{(i)}|\theta}(x^{(i)}|\theta) = \mathcal{N}(x^{(i)}; \mu, Q), \quad i = 1, \dots, \mathcal{M}, \quad (15)$$

where $\theta = (\mu, Q)$. For the parameter θ of this Gaussian density we assume some prior distribution $f_{\theta}(\theta)$. [Loe and Tjelmeland \(2021\)](#) assume a normal inverse Wishart prior for (μ, Q^{-1}) , which implies that Q is full, whereas we want to adopt a prior which ensures that Q is a band matrix. In [Section 4.1](#) we detail the prior we are using. The last element of the assumed model is to let the new data y be conditionally independent of $x^{(1)}, \dots, x^{(\mathcal{M})}$ and θ given x , and

$$f_{y|x}(y|x) = \mathcal{N}(y; Hx, R). \quad (16)$$

Based on the assumed model the goal is to construct a procedure for generating an updated version $\tilde{x}^{(m)}$ of $x^{(m)}$. One should first generate a $\theta = (\mu, Q)$ and thereafter $\tilde{x}^{(m)}$. In addition to being a function of $x^{(m)}$ it is natural to allow $\tilde{x}^{(m)}$ to depend on the generated θ and the new data y , as also indicated in the DAG in [Figure 2](#). The corresponding conditional distribution for $\tilde{x}^{(m)}$ we denote by $q(\tilde{x}^{(m)}|x^{(m)}, \theta, y)$. The updated $\tilde{x}^{(m)}$ is to be used as an (approximate) sample from $p(x_t|y_{1:t})$, which in the ensemble based setting we are considering here is represented by $p(x_t|x_t^{(1)}, \dots, x_t^{(\mathcal{M})}, y_t)$. However, as we want to use $x^{(m)}$ as a source for randomness when generating $\tilde{x}^{(m)}$, the $x^{(m)}$ must be removed from the conditioning set so one should instead consider $p(x_t|x_t^{(1)}, \dots, x_t^{(m-1)}, x_t^{(m+1)}, \dots, x_t^{(\mathcal{M})}, y_t)$. Under the assumed model this density is equal to $f_{x|z^{(m)}, y}(x|z^{(m)}, y)$ when using the shorthand notation $z^{(m)} = (x^{(1)}, \dots, x^{(m-1)}, x^{(m+1)}, \dots, x^{(\mathcal{M})})$. Thus, we should construct

$q(\tilde{x}^{(m)}|x^{(m)}, \theta, y)$ so that

$$f_{\tilde{x}^{(m)}|z^{(m)}, y}(x|z^{(m)}, y) = f_{x|z^{(m)}, y}(x|z^{(m)}, y) \quad (17)$$

holds for all values of x , $z^{(m)}$ and y . Loe and Tjelmeland (2021) show that (17) is fulfilled if $\tilde{x}^{(m)}$ is generated by first sampling $\theta = (\mu, Q)$ from $f_{\theta, z^{(m)}, y}(\theta|z^{(m)}, y)$ and thereafter $\tilde{x}^{(m)}$ is sampled according to a $q(\tilde{x}^{(m)}|x^{(m)}, \theta, y)$ defined by

$$\tilde{x}^{(m)} = B(x^{(m)} - \mu) + \mu + K(y - H\mu) + \tilde{\epsilon}^{(m)}, \quad (18)$$

where $\tilde{\epsilon}^{(m)}$ is independent of everything else and generated from a zero-mean Gaussian distribution with a covariance matrix S , B is a matrix connected to the positive semidefinite S by the relation

$$BQ^{-1}B^T + S = (I - KH)Q^{-1}, \quad (19)$$

and K is the Kalman gain matrix

$$K = (Q + H^T R H)^{-1} H^T R. \quad (20)$$

We note in passing that by inserting for K in (19) and thereafter applying the Woodbury identity (Woodbury, 1950), one gets $(I - KH)Q^{-1} = (Q + H^T R H)^{-1}$, so (19) is equivalent to

$$BQ^{-1}B^T + S = (Q + H^T R H)^{-1}. \quad (21)$$

3.2 Optimality criterion

When applying the updating equation (18) we have a freedom in the choice of the matrices B and S . The restrictions are that S must be positive semidefinite and that B and S should be related as specified by (21).

Under the assumed model all choices of B and S fulfilling the given restrictions are equally good, as they are all generating an $\tilde{x}^{(m)}$ from the same distribution. When recognising that the assumed model is wrong, however, all solutions are no longer equally good. So we should choose a solution which is robust against the assumptions made in the assumed model. Loe and Tjelmeland (2021) formulate a robust solution as one where the $x^{(m)}$ is changed as little as possible when forming $\tilde{x}^{(m)}$, under the condition that B and S satisfy (21). The intuition is that this should allow non-Gaussian properties in $x^{(m)}$ to be transferred to $\tilde{x}^{(m)}$. Mathematically the criterion is formulated as minimising the expected squared Euclidean distance between $x^{(m)}$ and $\tilde{x}^{(m)}$. Thus, we should minimise

$$\mathbb{E} \left[(x^{(m)} - \tilde{x}^{(m)})^T (x^{(m)} - \tilde{x}^{(m)}) \right], \quad (22)$$

Algorithm 1 Summary of the resulting updating procedure for computing the posterior ensemble $\tilde{x}^{(1)}, \dots, \tilde{x}^{(\mathcal{M})}$ from the prior ensemble $x^{(1)}, \dots, x^{(\mathcal{M})}$.

Given $x^{(1)}, \dots, x^{(\mathcal{M})}$, y , H and R .

For $m = 1, \dots, \mathcal{M}$:

1. Sample $\theta = (\mu, Q)$ from $f_{\theta|z^{(m)}, y}(\theta|z^{(m)}, y)$.
 2. Do singular value decomposition in (24): $VDV^T = Q$.
 3. Do singular value decomposition in (25): $U\Lambda U^T = Q + H^T R H$.
 4. Evaluate Z in (26): $Z = \Lambda^{-\frac{1}{2}} U^T V D^{-\frac{1}{2}}$.
 5. Do singular value decomposition in (26): $PGF^T = Z$.
 6. Evaluate B in (23): $B = U\Lambda^{-\frac{1}{2}} P F^T D^{\frac{1}{2}} V^T$.
 7. Evaluate $\tilde{x}^{(m)}$: $\tilde{x}^{(m)} = B(x^{(m)} - \mu) + \mu + K(y - H\mu)$
-

with respect to B and S under the restriction (21), where the expectation is with respect to the joint distribution of $x^{(m)}$ and $\tilde{x}^{(m)}$ under the assumed model. Note that [Loe and Tjelmeland \(2021\)](#) is considering a slightly more general solution by using a Mahalanobis distance. [Loe and Tjelmeland \(2021\)](#) show that (22) is minimised under the specified restrictions when $S = 0$ and

$$B = U\Lambda^{-\frac{1}{2}} P F^T D^{\frac{1}{2}} V^T, \quad (23)$$

where U and V are orthogonal matrices and D and Λ are diagonal matrices given by the singular value decompositions

$$Q = V D V^T, \quad (24)$$

$$Q + H^T R H = U \Lambda U^T, \quad (25)$$

and P and F are orthogonal matrices given by the singular value decomposition

$$Z = \Lambda^{-\frac{1}{2}} U^T V D^{-\frac{1}{2}} = P G F^T. \quad (26)$$

3.3 Resulting updating procedure

The resulting procedure for updating a prior ensemble $x^{(1)}, \dots, x^{(\mathcal{M})}$ to the corresponding posterior ensemble $\tilde{x}^{(1)}, \dots, \tilde{x}^{(\mathcal{M})}$ is summarised by the pseudocode in [Algorithm 1](#).

In the following sections our focus is on how to make this updating procedure computationally efficient when the dimensions of the state vector and corresponding observation vector are large. First, in [Section 4](#), we propose a new prior for θ which enables efficient sampling of $\theta = (\mu, Q)$ from the corresponding posterior $f_{\theta|z^{(m)}, y}(\theta|z^{(m)}, y)$. The generated Q is then a sparse matrix, which also limits the memory usage necessary to store it, since we of course only need to store the non-zero elements. However, sparsity of Q does not influence the computational efficiency of the singular value decompositions in [Steps 2, 3 and 5](#) of [Algorithm 1](#). One should note that we may

rephrase Steps 2 and 3 to use Cholesky decompositions instead, since Q and $Q + H^T R H$ are symmetric and positive definite matrices. Under reasonable assumptions also $Q + H^T R H$ is a sparse matrix so thereby these two steps can be done computationally efficient. The Z in Step 5, however, is in general neither a symmetric positive definite matrix, nor sparse. To introduce Cholesky decompositions in Steps 2 and 3 will therefore not change the order of the computational complexity of the procedure. Instead of substituting the singular value decompositions in Steps 2 and 3 with Cholesky decompositions, we therefore in Section 5 propose an approximation of Steps 2 to 6 by splitting the state vector into a series of blocks and running Steps 2 to 6 for each of the blocks separately.

4 Prior model and sampling of $\theta = (\mu, Q)$

In this section we first formulate the new prior for $\theta = (\mu, Q)$, where Q is restricted to be a band matrix. Thereafter we formulate a computationally efficient procedure to generate a sample from the resulting $f_{\theta|z^{(m)}, y}(\theta|z^{(m)}, y)$. We start by formulating the prior.

4.1 Prior for $\theta = (\mu, Q)$

To obtain a band structure for the precision matrix Q we restrict the assumed Gaussian distributions in (14) and (15) to be a Gaussian partially ordered Markov model, a Gaussian POMM (Cressie and Davidson, 1998). To be able to give a mathematically precise definition of the Gaussian POMM we first introduce some notation.

We let x^k denote the k 'th element of x , so $x = (x^1, \dots, x^{n_x})$. To each element x^k of x we associate a sequential neighbourhood $\Lambda_k \subseteq \{1, \dots, k-1\}$, and use the notation introduced in Section 2.2 to denote the elements in x associated to Λ_k by x^{Λ_k} . The number of elements in Λ_k we denote by $|\Lambda_k|$. Moreover, we let $\Lambda_k(1)$ denote the smallest element in the set Λ_k , we let $\Lambda_k(2)$ be the second smallest element in Λ_k , and so on until $\Lambda_k(|\Lambda_k|)$, which is the largest element in Λ_k . We let the distribution of x be specified by the two parameter vectors $\eta = (\eta^1, \dots, \eta^{n_x})$ and $\phi = (\phi^1, \dots, \phi^{n_x})$, where for each $k = 1, \dots, n_x$ we have that $\eta^k \in \mathbb{R}^{|\Lambda_k|+1}$ and $\phi^k > 0$ is a scalar. With this notation the Gaussian POMM is specified as

$$f_{x|\eta, \phi}(x|\eta, \phi) = \prod_{k=1}^{n_x} f_{x^k|\eta^k, \phi^k, x^{\Lambda_k}}(x^k|\eta^k, \phi^k, x^{\Lambda_k}), \quad (27)$$

where $x^k|\eta^k, \phi^k, x^{\Lambda_k}$ is Gaussian with mean

$$\begin{aligned} E[x^k|\eta^k, \phi^k, x^{\Lambda_k}] &= \eta^{k,1} + x^{\Lambda_k(1)}\eta^{k,2} + \dots + x^{\Lambda_k(|\Lambda_k|)}\eta^{k,|\Lambda_k|+1} \\ &= [1 \ (x^{\Lambda_k})^T] \eta^k \end{aligned} \quad (28)$$

and variance $\text{Var}[x^k | \eta^k, \phi^k, x^{\Lambda_k}] = \phi^k$.

It should be noted that $\theta = (\mu, Q)$ in $\mathcal{N}(x; \mu, Q)$ is uniquely specified by η and ϕ , and that the resulting Q is sparse. A derivation of the relation and a discussion of the sparseness of Q is included in Appendix A. We can therefore specify a prior for θ by specifying a prior for η and ϕ , which we choose as conjugate to the Gaussian POMM just defined. More specifically, we first assume the elements in ϕ to be independent, and each element ϕ^k to be inverse Gamma distributed with parameters α^k and β^k . Next, we assume the elements of η to be conditionally independent and Gaussian distributed given ϕ ,

$$\eta^k | \phi \sim \mathcal{N}(\eta^k; \zeta^k, (\phi^k \Sigma_{\eta^k})^{-1}), \quad (29)$$

where $\zeta^k \in \mathbb{R}^{|\Lambda_k|+1}$ and $\Sigma_{\eta^k} \in \mathbb{R}^{(|\Lambda_k|+1) \times (|\Lambda_k|+1)}$ are hyperparameters that have to be set.

4.2 Sampling from $f_{\theta|z^{(m)}, y}(\theta|z^{(m)}, y)$

To sample from $f_{\theta|z^{(m)}, y}(\theta|z^{(m)}, y)$ we adopt the same general strategy as proposed in Loe and Tjelmeland (2021). We include the underlying state vector at time t , x , as an auxiliary variable and simulate (θ, x) from

$$\begin{aligned} f_{\theta, x|z^{(m)}, y}(\theta, x|z^{(m)}, y) &\propto f_{\theta}(\theta) f_{x|\theta}(x|\theta) f_{y|x}(y|x) \prod_{i \neq m} f_{x^{(i)}|\theta}(x^{(i)}|\theta) \\ &= f_{\theta}(\theta) \mathcal{N}(x; \mu, Q) \mathcal{N}(y; Hx, R) \prod_{i \neq m} \mathcal{N}(x^{(i)}; \mu, Q). \end{aligned} \quad (30)$$

By thereafter ignoring the simulated x we have a sample of θ from the desired distribution. To simulate from the joint distribution $f_{\theta, x|z^{(m)}, y}(\theta, x|z^{(m)}, y)$ we adopt a two block Gibbs sampler, alternating between drawing x and θ from the full conditionals $f_{x|\theta, z^{(m)}, y}(x|\theta, z^{(m)}, y)$ and $f_{\theta|x, z^{(m)}, y}(\theta|x, z^{(m)}, y)$, respectively. We initialise the Gibbs sampler by setting $x = \frac{1}{M-1} \sum_{i \neq m} x^{(i)}$. This initial value should be centrally located in $f_{x|z^{(m)}, y}(x|z^{(m)}, y)$, and since the Gibbs sampler we are using only consists of two blocks we should expect it to converge very fast. So just a few iterations should suffice.

From (30) we get the full conditional for x

$$f_{x|\theta, z^{(m)}, y}(x|\theta, z^{(m)}, y) = f_{x|\theta, y}(x|\theta, y) \propto \mathcal{N}(x; \mu, Q) \mathcal{N}(y; Hx, R). \quad (31)$$

It is straightforward to show that this is a Gaussian distribution with mean $\tilde{\mu}$ and covariance matrix \tilde{Q} given by

$$\tilde{\mu} = \mu + (Q + H^T R H)^{-1} H^T R (y - H\mu), \quad (32)$$

$$\tilde{Q} = Q + H^T R H. \quad (33)$$

With the chosen prior for θ , Q is sparse and if x represents values in a two dimensional lattice and the sequential neighbourhoods Λ_k are chosen as translations of each other, as we use in the simulation example in Section 6, the Q is a band matrix. As also mentioned above, the detailed sparseness structure of Q we discuss in Appendix A. Assuming also R and H to be band matrices, the product $H^T R H$ can be efficiently computed and is also a band matrix. The \tilde{Q} is thereby also a band matrix, so the Cholesky decomposition of it can be computed efficiently as discussed in Section 2.1. The band structures of H and R can be used to evaluate the right hand side of (32) efficiently, and in addition computational efficiency can be gained by computing the product $H^T R(y - H\mu)$ in the right order. In general, multiplying two matrices $C \in \mathbb{R}^{u \times v}$ and $D \in \mathbb{R}^{v \times w}$ has computational complexity $\mathcal{O}(uvw)$. Hence, we should first compute $R(y - H\mu)$ before calculating $H^T R(y - H\mu)$. Having \tilde{Q} and the Cholesky decomposition of \tilde{Q} we can both get $\tilde{\mu}$ and generate a sample from the Gaussian distribution efficiently as discussed in Section 2.1.

From (30) we also get the full conditional for θ ,

$$\begin{aligned} f_{\theta|x, z^{(m)}, y}(\theta|x, z^{(m)}, y) &= f_{\theta|x, z^{(m)}}(\theta|x, z^{(m)}) \\ &\propto f_{\theta}(\theta) \mathcal{N}(x; \mu, Q) \prod_{i \neq m} \mathcal{N}(x^{(i)}; \mu, Q). \end{aligned} \quad (34)$$

To simulate from this full conditional we exploit that $\theta = (\mu, Q)$ is uniquely given by the parameters ϕ and η of the Gaussian POMM prior, which means that we can first simulate values for ϕ and η from $f_{\phi, \eta|x, z^{(m)}}(\phi, \eta|x, z^{(m)})$ and thereafter use the generated ϕ and η to compute the corresponding μ and Q . In Appendix B we study in detail the resulting $f_{\phi, \eta|x, z^{(m)}}(\phi, \eta|x, z^{(m)})$ and show that it has the same form as the corresponding prior $f_{\phi, \eta}(\phi, \eta)$, but with updated parameters. More specifically, the elements of ϕ are conditionally independent given x and $z^{(m)}$, with

$$\phi^k | z^{(m)}, x \sim \text{InvGam}(\tilde{\alpha}^k, \tilde{\beta}^{(m), k}), \quad (35)$$

where

$$\tilde{\alpha}^k = \alpha^k + \frac{\mathcal{M}}{2}, \quad (36)$$

$$\tilde{\beta}^{(m), k} = \left(\frac{1}{\beta^k} + \frac{1}{2} (\gamma^{(m), k} - (\rho^{(m), k})^T (\Theta^{(m), k})^{-1} \rho^{(m), k}) \right)^{-1}, \quad (37)$$

$$\gamma^{(m), k} = (\zeta^k)^T \Sigma_{\eta^k}^{-1} \zeta^k + (\chi^{(m), k})^T \cdot \chi^{(m), k}, \quad (38)$$

$$\rho^{(m), k} = \Sigma_{\eta^k}^{-1} \zeta^k + (1, (\chi^{(m), \Lambda_k})^T)^T \cdot (\chi^{(m), k})^T, \quad (39)$$

$$\Theta^{(m), k} = \Sigma_{\eta^k}^{-1} + (1, (\chi^{(m), \Lambda_k})^T)^T \cdot (1, (\chi^{(m), \Lambda_k})^T) \quad (40)$$

and

$$\chi^{(m),k} = (x^{(1),k}, \dots, x^{(m-1),k}, x^{(m+1),k}, \dots, x^{(\mathcal{M}),k}, x^k), \quad (41)$$

$$\chi^{(m),\Lambda_k} = (x^{(1),\Lambda_k}, \dots, x^{(m-1),\Lambda_k}, x^{(m+1),\Lambda_k}, \dots, x^{(\mathcal{M}),\Lambda_k}, x^{\Lambda_k}). \quad (42)$$

The distribution for η given ϕ , x and $z^{(m)}$ becomes

$$f_{\eta|\phi, z^{(m)}, x}(\eta|\phi, z^{(m)}, x) = \prod_{k=1}^{n_x} f_{\eta^k|\phi^k, z^{(m)}, x}(\eta^k|\phi^k, z^{(m)}, x) \quad (43)$$

where

$$\eta^k|\phi^k, z^{(m)}, x \sim \mathcal{N}(\eta^k; (\Theta^{i,k})^{-1}\rho^{i,k}, (\phi^k)^{-1}\Theta^{i,k}). \quad (44)$$

In particular we see that it is easy to sample from $f_{\phi, \eta|x, z^{(m)}}(\phi, \eta|x, z^{(m)})$ by first sampling the elements of ϕ independently according to (35) and thereafter generate the elements of η according to (44). Having samples of ϕ and η we can thereafter compute the corresponding μ and Q as detailed in Appendix A.

5 Block update

Section 3 presents a set of updating procedures that allows us to update a prior realisation into a posterior realisation, where the posterior realisation takes the observation in the current time step into account. In Section 3.2, we found the optimal filter according to our chosen criterion. However, as also discussed in Section 3.3, parts of this procedure is computationally demanding. In the following we introduce the approximate, but computationally more efficient procedure for Steps 2 to 6 in Algorithm 1 that we mentioned in Section 3.3. So the situation considered is that we already have generated a mean vector μ and a sparse precision matrix Q , and the goal is now to define an approximation to the matrix B given in Step 6 in Algorithm 1. The strategy is then to use the approximation to B , which we denote by $B^* \in \mathbb{R}^{n_x \times n_x}$, instead of the exact matrix B when we perform Step 7 in Algorithm 1. In the following we also assume the matrices H and R to be sparse.

Our construction of B^* is general, but to motivate our construction of B^* we consider a situation where the elements of the state vector are related to nodes in a two-dimensional (2D) lattice of nodes, with r rows and s columns say, and where the correlation between two elements of the state vector decay with distance between the corresponding nodes. We assume the nodes in the lattice to be numbered in the lexicographical order, so node (k, ℓ) in the lattice is related to the value of element number $(k-1) \cdot s + \ell$ of the state vector. We use $\mathcal{S} = \{(k, \ell) : k = 1, \dots, r, \ell = 1, \dots, s\}$ to denote the set of all indices of the elements in the state vector, where we for the 2D lattice example have $n_x = rs$.

The first step in the construction of B^* is to define a partition $C_1, \dots, C_{\mathcal{B}}$ of \mathcal{S} . The sets $C_b, b = 1, \dots, \mathcal{B}$ should be chosen so that the corresponding elements of the state vector are highly correlated. In the 2D lattice example

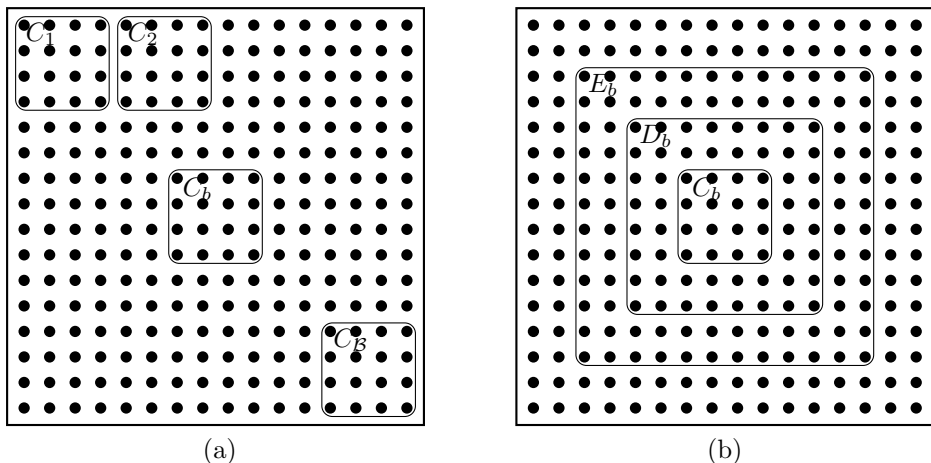


Fig. 3 Example of how the sets C_b , D_b and E_b can be chosen when the elements of x are related to the nodes of a 2D lattice. The dots denote nodes. In (a) the nodes are partitioned in \mathcal{B} different blocks, while (b) shows an example of how D_b and E_b might look like

the most natural choice would be to let each C_b be a block of consecutive nodes in the lattice, for example a block of $r_C \times s_C$ nodes. Such a choice of the partition is visualised in Figure 3(a). One should note that a similar partition of \mathcal{S} is also used in the domain localisation version of EnKF (Janjic et al, 2011). However, the motivation for the partition in domain localisation is mainly to eliminate or at least reduce the effect of spurious correlations (Haugen and Evensen, 2002), whereas in our setup the motivation is merely to reduce the computational complexity of the updating procedure. In particular, if the dimension of the state vector, n_x , is sufficiently small we recommend not to use the block updating procedure at all, one should then use the procedure summarised in Section 4.

One would naturally expect that an element (k, ℓ) of the matrix B , $B_{k\ell}$, is close to zero whenever the correlation between the corresponding elements in the state vector is essentially zero. In numerical experiments where the dimension of the state vector is sufficiently small so that we can use the procedure in Section 3.3 to compute B , this intuition has already been confirmed. Our first approximation is therefore to set such elements in B^* exactly equal to zero. More formally, for each $b = 1, \dots, \mathcal{B}$ we define a set of nodes D_b so that $C_b \subseteq D_b$, and set $B_{k\ell}^* = 0$ for all $k \in C_b, \ell \notin D_b$. In the 2D lattice example it is natural to define D_b by expanding the C_b block of nodes with u , say, nodes in each direction, see the illustration in Figure 3(b) where $u = 2$ is used.

To decide the value of the elements of B^* that is related to block C_b and that has not been set to zero, i.e. $B_{k\ell}^*, k \in C_b, \ell \in D_b$, the most natural procedure would be the following. Start with the assumed joint Gaussian distribution for the state vector x and the observation vector y , and then marginalise out all elements of the state vector that are not in D_b . One would then have ended up with the joint normal distribution for the elements of the

state vector x related to the block D_b and the observation vector y . From this, one could find the marginal distribution for the elements of the state vector x related to the block D_b , and the conditional distribution for the observation vector y given the elements of the state vector related to D_b . One could then use the procedure specified in Section 3.3 to find the optimal B matrix for the reduced problem, and thereafter picked out all elements in rows corresponding to elements in C_b in this B matrix and put these values into the corresponding place in the B^* matrix. However, such a procedure is not computationally feasible when the dimension of the state vector is large, and for two reasons. First, the marginalisation over all the elements of the state vector that are not in D_b is computationally expensive when dependence is represented by precision matrices. Second, when the dimension of the state vector is large the dimension of the observation vector y is typically also large, which makes the marginalisation process even more computationally expensive. We therefore do one more approximation before following the procedure described. Instead of starting out with the joint distribution for the state vector x and the observation vector y , we start with the corresponding conditional distribution where we condition on some elements of the state and observation vectors that are only weakly correlated with the elements of the state vector in D_b to be equal to their respective mean values. In the following, we define this last approximation more formally.

For each $b = 1, \dots, \mathcal{B}$, we define a set of nodes E_b such that $D_b \subseteq E_b$. The set E_b should be chosen so that the nodes in D_b are weakly correlated with the nodes that are not in E_b . For the 2D lattice example it is reasonable to define E_b by expanding the D_b block with, say, v nodes in each direction. Figure 3(b) displays an example of E_b where $v = 2$. We use the notation introduced in Section 2.2 and denote the elements of the state vector related to the block E_b as x^{E_b} . Similarly, we denote elements of x not related to E_b as x^{-E_b} . Moreover, we define a set J_b , which contains the indices of the elements in y that are linked to x^{E_b} . An element y^k is linked to x^{E_b} if $H^{k,\ell} \neq 0$ for at least one element $\ell \in E_b$, where we recall that H comes from (16). In the following, we find the corresponding values for μ, Q, H and R that we use in Algorithm 1. We start by forming the joint Gaussian distribution of the state vector x and the observations y .

We have that

$$f_{x,y|\theta}(x, y|\theta) = f_{x|\theta}(x|\theta) f_{y|x}(y|x). \quad (45)$$

Further on, we set x^k equal to its mean value μ^k for all $k \notin E_b$, and y^k equal to its conditional mean value $(Hx)^k$ for all $k \notin J_b$. The resulting conditional distribution we denote by

$$g(x^{E_b}, y^{J_b}|\theta) = f(x^{E_b}, y^{J_b}|\theta, x^{-E_b} = \mu^{-E_b}, y^{-J_b} = (Hx)^{-J_b}), \quad (46)$$

which is also multivariate Gaussian. The distribution $g(x^{E_b}, y^{J_b}|\theta)$ is computed using the expressions presented in Section 2.2. Note that when we condition on $x^{-E_b} = \mu^{-E_b}$ and $y^{-J_b} = (Hx)^{-J_b}$ some of the entries of x, y, μ, Q, H

and R vanish from the expression. In the following, we compute $g(x^{D_b}|\theta)$ and $g(y^{J_b}|x^{D_b}, \theta)$ based on $g(x^{E_b}, y^{J_b}|\theta)$.

From $g(x^{E_b}, y^{J_b}|\theta)$ we marginalise over $x^{E_b \setminus D_b}$ to get $g(x^{D_b}, y^{J_b}|\theta)$, which is also Gaussian and where the mean vector and the precision matrix can be found as discussed in Section 2.2. From $g(x^{D_b}, y^{J_b}|\theta)$ we in turn find $g(x^{D_b}|\theta)$ and $g(y^{J_b}|x^{D_b}, \theta)$, which are also Gaussian and where the mean vectors and the precision matrices can again be found using the expressions in Section 2.2. The parameters in $g(x^{D_b}|\theta)$ and $g(y^{J_b}|x^{D_b}, \theta)$ can be used in Steps 2 to 8 of Algorithm 1 to compute the corresponding optimal B matrix for the update of x^{D_b} . As discussed above, one should then pick out all elements corresponding to the elements in C_b in this B matrix for x^{D_b} and put these values into the corresponding place in the approximate B^* matrix. In the computation of Steps 2 to 6 in Algorithm 1, the mean vector and the precision matrix in $g(x^{D_b}|\theta)$ should be used as μ and Q , respectively. The likelihood is now $g(y^{J_b}|x^{D_b}, \theta)$, so the precision matrix of this distribution should be used as R in Algorithm 1. The conditional mean in $g(y^{J_b}|x^{D_b}, \theta)$ is on the form $E[y^{J_b}|x^{D_b}, \theta] = a + Lx^{D_b}$, whereas Algorithm 1 is based on a likelihood where the conditional mean is without a constant term. We must therefore use that to condition on the value of y^{D_b} is equivalent to condition on the value of $y^{D_b} - a$. In Algorithm 1, L and $y^{D_b} - a$ should therefore be used as H and y , respectively.

6 Simulation example

In the following we present a numerical experiment where we compare the optimal model-based EnKF procedure from Section 3.3 with the block update procedure introduced in Section 5. The purpose of the experiment is twofold, to study the computational speedup resulting from using the block update, and to study the quality of the resulting approximation. We first generate a series of reference states $\{x_t\}_{t=1}^T$ and corresponding observed values $\{y_t\}_{t=1}^T$. The series of reference states we consider as the unknown true values of the latent x_t process and we use the corresponding generated observed values in the two versions of EnKF. We then compare the computational demands and the output of the two filtering procedures.

6.1 Reference time series and observations

To generate the series of reference states we adopt a two dimensional variant of the one dimensional setup used in Omre and Myrseth (2010). So for each time step $t = 1, \dots, T$ the reference state x_t represents the values in a two dimensional $s \times s$ lattice. As described in Section 5 we number the nodes in the lexicographical order. The reference state at time $t = 1$ we generate as a moving average of a white noise field. More precisely, we first generate independent and standard normal variates $z^{(k, \ell)}$ for each node (k, ℓ) , and to avoid boundary effects we do this for an extended lattice. The reference state

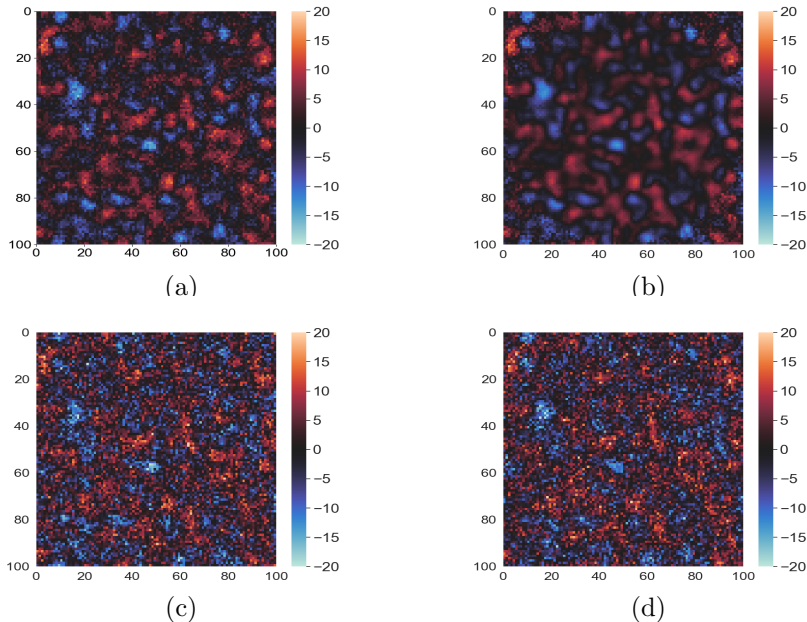


Fig. 4 Reference states at times (a) $t = 1$ and (b) $t = 5$, and corresponding generated observed values at times (c) $t = 1$ and (d) $t = 5$

at node (k, ℓ) and time $t = 1$ is then defined by

$$x_1^{(k-1) \cdot s + \ell} = \sqrt{\frac{20}{|\Gamma_{3,(k,\ell)}|}} \sum_{(i,j) \in \Gamma_{3,(k,\ell)}} z^{(i,j)}, \quad (47)$$

where $\Gamma_{r,(k,\ell)}$ is the set of nodes in the extended lattice, that are less than or equal to a distance r from node (k, ℓ) , and $|\Gamma_{r,(k,\ell)}|$ is the number of elements in that set. One should note that the factor $\sqrt{20/|\Gamma_{3,(k,\ell)}|}$ gives that the variance of each generated $x_1^{(k-1) \cdot s + \ell}$ is 20. Figure 4(a) shows a generated x_1 with $s = 100$, which is used in the numerical experiments discussed in Sections 6.4 and 6.5.

Given the reference state at time $t = 1$, corresponding reference states at later time steps are generated sequentially. For $t = 2, \dots, T$ the reference state at time $t - 1$ is used to generate the reference state at time t by performing a moving average operation on nodes that are inside an annulus defined by circles centered at the middle of the lattice. For $t = 2$ the radius of the inner circle defining the annulus is zero, and as t increases the annulus is gradually moved further away from the center. More precisely, to generate x_t from x_{t-1} we define the annulus by the two radii $r_1 = \max\{0, \lfloor (\frac{s}{2} - 1) \frac{1}{T-1} (t - \frac{5}{2}) \rfloor\}$ and $r_2 = \lfloor (\frac{s}{2} - 1) \frac{t-1}{T-1} \rfloor$, where $\lfloor v \rfloor$ denotes the largest integer less than or

equal to v . For all nodes (k, ℓ) inside the annulus we define

$$x_t^{(k-1) \cdot s + \ell} = \frac{1}{|\Gamma_{1, (k, \ell)}|} \sum_{(i, j) \in \Gamma_{1, (k, \ell)}} x_{t-1}^{(i-1) \cdot s + j}. \quad (48)$$

For nodes (k, ℓ) that are not inside the specified annulus the values are unchanged, i.e. for such nodes we have $x_t^{(k-1) \cdot s + \ell} = x_{t-1}^{(k-1) \cdot s + \ell}$. The reference solution at time $T = 5$ corresponding to the x_1 given in Figure 4(a) is shown in Figure 4(b). By comparing the two we can see the effect of the smoothing operations.

For each time step $t = 1, \dots, T$ we generate an observed value associated to each node in the lattice, so $n_y = n_x$. We generate the observed values at time t , y_t , by blurring x_t and adding independent Gaussian noise in each node. More precisely, the observed value in node (k, ℓ) at time t is generated as

$$y_t^{(k-1) \cdot s + \ell} = \frac{1}{|\Gamma_{\sqrt{2}, (k, \ell)} \cap \mathcal{S}|} \sum_{(i, j) \in \Gamma_{\sqrt{2}, (k, \ell)} \cap \mathcal{S}} x_t^{(i-1) \cdot s + j} + w^{(k-1) \cdot s + \ell}, \quad (49)$$

where $w^{(k-1) \cdot s + \ell}$ is a zero-mean normal variate with variance 20. Figures 4(c) and 4(d) shows the generated observations corresponding to the x_1 and x_5 in Figures 4(a) and (b), respectively. These observations are used in the numerical experiments discussed in Sections 6.4 and 6.5.

6.2 Assumed model and algorithmic parameters

In the numerical experiments with EnKFs we use the assumed model defined in Section 3.1. For nodes sufficiently far away from the lattice borders we let the sequential neighbourhood consist of ten nodes as shown in Figure 5.

This set of sequential neighbours should be sufficient to be able to represent a large variety of spatial correlation structures at the same time as it induces sparsity in the resulting precision matrix. For nodes close to the lattice borders we reduce the number of sequential neighbours to consist of only the subset of the ten nodes shown in Figure 5 that are within the lattice.

As priors for η and ϕ we use the parametric forms specified in Section 4.1. We want these priors to be vague so that the resulting posterior distributions are mainly influenced by the prior ensemble. We let the prior for ϕ be improper by setting $\alpha^k = 0$ and $\beta^k = \infty$ for all k . In the prior for $\eta_k | \phi_k$ we set $\zeta^k = 0$ and $\Sigma_{\eta^k} = 100 \cdot I_{|\Lambda_k|+1}$ for all k .

In preliminary simulation experiments we found that the Gibbs sampler for the sampling of θ converged very rapidly, consistent with our discussion in Section 4.2. In the numerical experiments we therefore only used five iterations of the Gibbs sampler. When using the block update procedure we let each C_b consist of a block of 20×20 nodes. To define the corresponding sets D_b and E_b we follow the procedure outlined in Section 5 with $u = v = 5$.

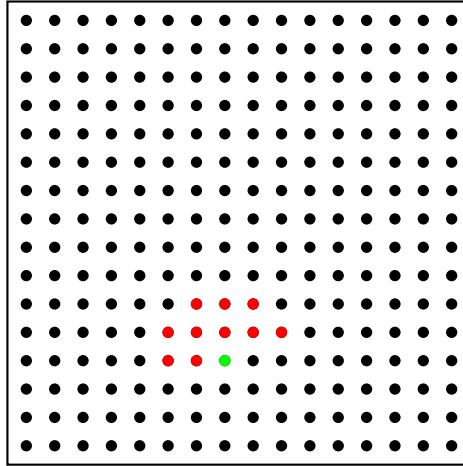


Fig. 5 The sequential neighbourhood used in the numerical examples. The red dots denote the sequential neighbours of the green node

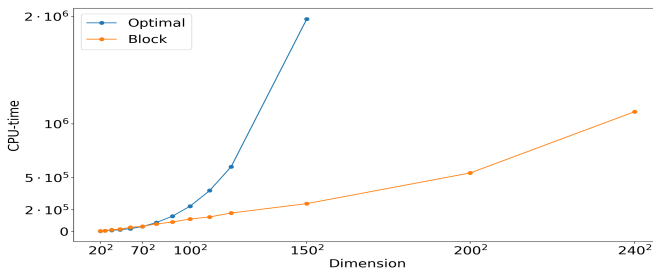


Fig. 6 Computing time used for running each of the two model-based EnKF procedures with $\mathcal{M} = 25$ ensemble elements for $T = 5$ time steps as a function of the number of nodes $n_x = s^2$ in the lattice. Computing time for the optimal model-based EnKF procedure is shown in blue, and corresponding computing time for the block updating procedure is shown in orange

6.3 Comparison of computational demands

The main objective of the block update procedure is to provide a computationally efficient approximation to the optimal model-based EnKF procedure defined in Section 3. In this section we compare the computational demands of the two updating procedures as a function of the number of nodes in the lattice.

For an implementation in Python, we run the two EnKF updating procedures discussed above with $\mathcal{M} = 25$ ensemble elements for $T = 5$ time steps for different lattice sizes and monitor the computing time used in each case. The results are shown in Figure 6. The observed computing times are shown as dots in the plot, in blue for the optimal model-based EnKF procedure and in orange for the block updating procedure. The lines between the dots are

just included to make it easier to read the plot. As we should expect from the discussion in Section 5 we observe that the speedup resulting from adopting the block update increases quickly with the lattice size.

6.4 Approximation error resulting from one block update

When adopting the block update in an EnKF procedure we will clearly get an approximation error in each update. When assessing this approximation error it is important to realise that the approximation error in one update may influence the behaviour of the filter also in later iterations. First, the effect of the approximation error emerged in one update may change when later iterations of the filter is run, the error may increase or decrease when run through later updates. Second, since the EnKF we are using is a stochastic filter, with the stochasticity lying in the sampling of θ , even a small change after one update may have a large impact on the resulting values in later iterations. In particular it is important to note that even if the approximation error in one update only marginally change the distribution of the values generated in later iterations, it may have a large impact on the actually sampled values. In this section our focus is to assess the approximation error in one update when using the block update, whereas in the next section we concentrate on the accumulated effect of the approximations after several iterations.

Adopting the reference time series and the data described in Section 6.1 and the assumed model and algorithmic parameters defined in Section 6.2 we isolate the approximation error in one update by the following procedure. We first run the optimal model-based EnKF procedure for all $T = 5$ steps. Thereafter, for each $t = 1, \dots, T$, we start with the prior ensemble generated for that time step in the optimal model-based EnKF and perform one step with the block update. One should note that since we are using the same prior ensemble for the block update as for the optimal model-based EnKF the generated parameters θ are identical for both updates, so the resulting difference in the updated values are only due to the difference in the B matrix used in the two procedures.

Figure 7 shows results for the nodes $(50, \ell)$, $\ell = 1, \dots, 100$ at time step $t = 4$. The ensemble averages and bounds of the empirical 90% prediction intervals for the optimal model-based EnKF procedure are shown in blue, and the corresponding values when using the block update procedure for time $t = 4$ are shown in dashed orange. For comparison the reference is shown in black. One can observe that for most nodes the mean value and interval bounds when using the block update are visually indistinguishable from the corresponding values when using the block update. The largest difference can be observed for the lower bound of the prediction interval for $\ell = 80$. Remembering that we are using blocks of 20×20 nodes in the block update it should not come as a surprise that the largest errors are for values of ℓ that are multiples of 20.

To study the approximation errors in more detail and in particular how the block structure used in the block update influence the approximation, we in Figure 8 show, for each $t = 1, \dots, 5$, the difference between the averages

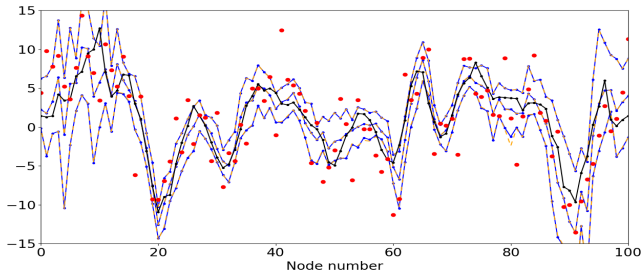


Fig. 7 Assessment of the approximation error by using the block update at step $t = 4$. The figure shows values for nodes $(50, \ell), \ell = 1, \dots, 100$. The values of the reference are shown in black and the observations at $t = 4$ are shown in red. The ensemble averages and bounds for the empirical 90% prediction intervals when using the optimal model-based EnKF are shown in blue. The corresponding ensemble averages and bounds for the empirical 90% prediction intervals when using the block update are shown in dashed orange

of the ensembles when using the optimal model-based EnKF and when using the block update procedure. As one should expect we see that the largest differences occur along the borders of the 20×20 blocks used in the block update. We can, however, also observe that the magnitude of the errors are all small compared with the spatial variability of the underlying x_t process, which explains why the approximation errors are almost invisible in Figure 7.

6.5 Accumulated approximation error versus Monte Carlo variability

In this section our focus is on assessment of the accumulated effect of the approximation error over several iterations. To do this we again adopt the reference time series, the data described in Section 6.1 and the assumed model and algorithmic parameters defined in Section 6.2. Based on this we run each of the optimal model-based EnKF and the block update procedures several times, each time with a different initial ensemble and using different random numbers in the updates. For two runs with each of the two filters, Figure 9 shows in green the values of all the $\mathcal{M} = 25$ ensemble elements in nodes $(50, \ell), \ell = 1, \dots, 100$ at time $T = 5$. The reference state at $T = 5$ is shown in black and the observations at time $T = 5$ are again shown as red dots. Figures 9(a) and (c) show results for the optimal model-based EnKF, whereas Figures 9(b) and (d) show results for the proposed block update procedure. Since all four runs are based on the same observations they obviously have many similarities. However, all the ensembles are different. Ensembles updated with the same updating procedure differ because of Monte Carlo variability, i.e. because they used different initial ensembles and different random numbers in the updates. When comparing an ensemble updated with the optimal model-based EnKF procedure with an ensemble updated with the block update, they differ both because of Monte Carlo variability and because of the accumulated effect of the approximation errors up to time T . In Figure 9, however, the

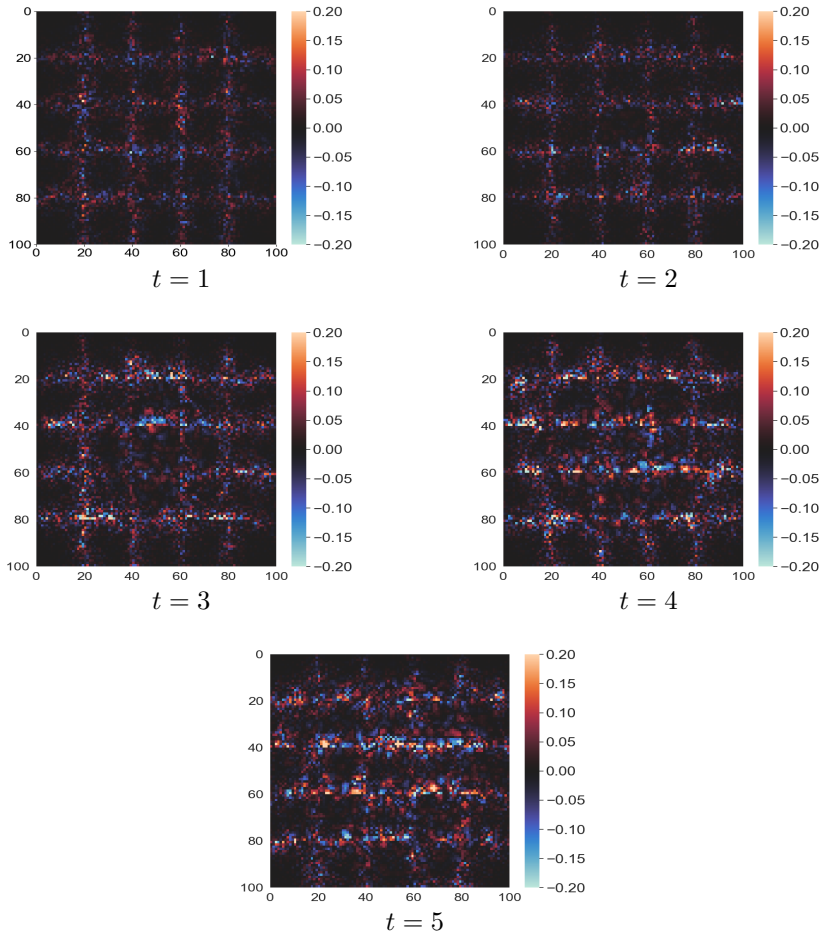


Fig. 8 Difference between the averages of the ensembles when using the optimal model-based EnKF and when using the block update. Results are shown for each $t = 1, \dots, 5$

differences between the ensembles in (a) and (b) and between the ensembles in (c) and (d) seem similar to the differences between the ensembles in (a) and (c) and between the ensembles in (b) and (d). So this indicates that the accumulated effect of the approximation error is small compared to the Monte Carlo variability.

To compare the magnitude of the accumulated approximation error with the Monte Carlo variability in more detail we adopt the two-sample Kolmogorov-Smirnov statistics to measure the difference between the values of two ensembles in one node. More precisely, letting $\widehat{F}_1(x; k, \ell)$ and $\widehat{F}_2(x; k, \ell)$ denote the empirical distribution functions for the values in node (k, ℓ) in two

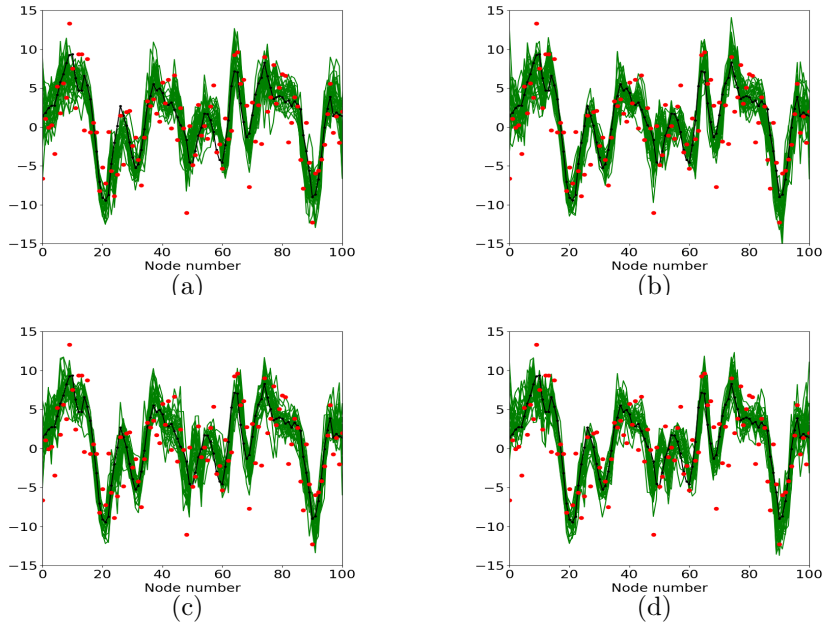


Fig. 9 The reference solution (black) and the observations (red) along one cross section of the grid at time $T = 5$. The green lines are the ensemble elements along the same cross section. Figures (a) and (c) show two simulations from the optimal update procedure, while (b) and (d) display two simulations from the block update

ensembles we use

$$D(k, \ell) = \max_x |\widehat{F}_1(x; k, \ell) - \widehat{F}_2(x; k, \ell)| \quad (50)$$

to measure the difference between the two ensembles at node (k, ℓ) . One should note that since we are using $\mathcal{M} = 25$ elements in each ensemble the $D(k, \ell)$ is a discrete variable with possible values $0.04d$; $d = 0, 1, \dots, 25$. Using three runs based on the optimal model-based EnKF we compute $D(k, \ell)$ for each possible pair of ensembles, for each $t = 1, \dots, 5$ and for each node in the 100×100 lattice. In Figure 10 histogram of the resulting 30 000 values for each $t = 1, \dots, 5$ are shown in blue. Correspondingly we estimate the distribution of $D(k, \ell)$ when one of the ensembles is based on the optimal model-based EnKF and the other is using the block update, and this is shown in red in Figure 10. Comparing the blue and the red histograms for each $t = 1, \dots, 5$ in Figure 10 one may arguably see a tendency of the mass in the orange histograms to be slightly moved to the right relative to the corresponding blue histograms. This is as one would expect, but we also observe that the effect of the approximation error is negligible compared to the Monte Carlo variability.

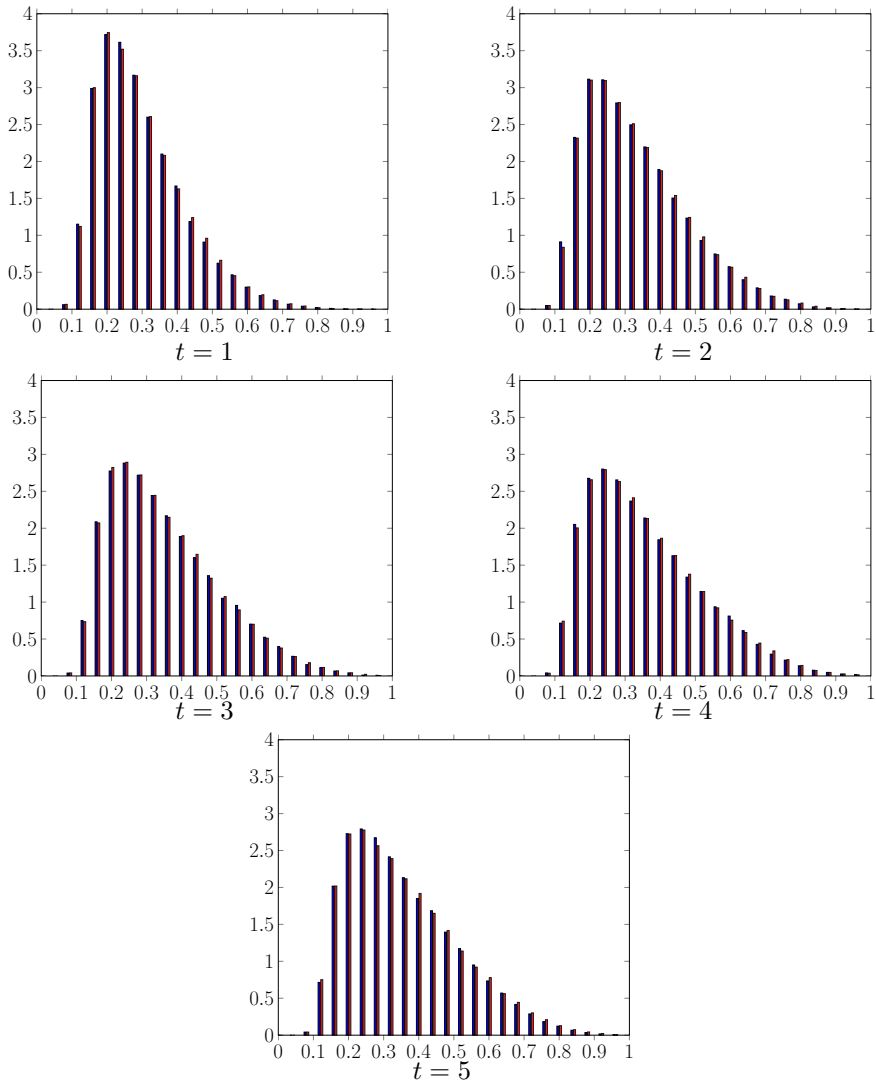


Fig. 10 Histograms of the two-sample Kolmogorov-Smirnov statistics. The statistics computed from two ensembles updated with the optimal ensemble are displayed in blue, while the statistics computed by two ensembles from different updating procedures are visualised in red

7 Closing remarks

In this paper we propose two changes in the model-based EnKF procedure introduced in [Loe and Tjelmeland \(2021\)](#). Our motivation is to get a procedure that is computationally faster than the original one, so that it is feasible to use it also in situations with high dimensional state vectors. The first change we introduce is to formulate the assumed model in terms of precision matrices

instead of covariance matrices, and to adopt a prior for the precision matrix that ensures the sampled precision matrices to be sparse. The second change we propose is to adopt the block update, which allows us to do singular value decompositions of many smaller matrices instead of for one large one.

In a simulation example we have studied both the computational speedup and the associated approximation error resulting when adopting the proposed procedure. The computational speedup is substantial for high dimensional state vectors and this allows the proposed filter to be run on much larger problems than can be done with the original formulation. At the same time the approximation error resulting from using the introduced block updating is negligible compared to the Monte Carlo variability inherent in both the original and the proposed procedures.

In order to further investigate the strengths and weaknesses of the proposed approach, it should be applied on more examples. It is of interest to gain more experience with the proposed procedure both in other simulation examples and in real data situations. In particular it is of interest to experiment more with different sizes for the C_b , D_b and E_b blocks to try to find the best sizes for these when taking both the computational time and the approximation quality into account. As for all EnKFs the proposed procedure is ideal for parallel computation and with an implementation more tailored for parallelisation it should be possible get a code that is running much faster than our more basic implementation.

Funding. Geophysics and Applied Mathematics in Exploration and Safe production (GAMES) at NTNU (Research Council of Norway; Grant No. 294404).

Declarations

Conflict of interest. No conflicts of interest.

Competing interests. The authors have no competing interests to declare that are relevant to the content of this article.

Appendices

A Derivation of $\theta = (\mu, Q)$ from ϕ and η

To find how $\theta = (\mu, Q)$ is given from ϕ and η we restrict the Gaussian densities $f(x|\theta)$ and $f(x|\phi, \eta)$ to be identical. The density $f(x|\theta)$ is given by

$$\begin{aligned} f(x|\theta) &\propto \exp \left\{ -\frac{1}{2}(x - \mu)^T Q (x - \mu) \right\} = \exp \left\{ -\frac{1}{2}x^T Q x + \mu^T Q x \right\} \\ &= \exp \left\{ \sum_{k=1}^{n_x} \left(-\frac{1}{2}Q^{k,k} \right) (x^k)^2 + \sum_{\ell < k} (-Q^{k,\ell}) x^k x^\ell + \sum_{k=1}^{n_x} \left(\sum_{\ell=1}^{n_x} \mu^\ell Q^{\ell,k} \right) x^k \right\}. \end{aligned} \quad (51)$$

Using the definition of $f(x|\phi, \eta)$ from Section 4.1 we have

$$\begin{aligned}
f(x|\phi, \eta) &= \prod_{k=1}^{n_x} f(x^k | x^{\Lambda_k}, \eta^k, \phi^k) \\
&\propto \prod_{k=1}^{n_x} \exp \left\{ -\frac{1}{2\phi^k} (x^k - (1, (x^{\Lambda_k})^T) \cdot \eta^k)^2 \right\} \\
&= \exp \left\{ -\frac{1}{2} \sum_{k=1}^{n_x} \frac{1}{\phi^k} \left(x^k - \eta^{k,1} - \sum_{\ell=2}^{|\Lambda_k|} \eta^{k,\ell} x^{\Lambda_k(\ell)} \right)^2 \right\} \\
&\propto \exp \left\{ \sum_{k=1}^{n_x} \left(-\frac{1}{2\phi^k} - \frac{1}{2} \sum_{\ell:k \in \Lambda_\ell} \frac{1}{\phi^\ell} \left(\eta^{\ell, \Lambda_\ell^{-1}(k)+1} \right)^2 \right) (x^k)^2 \right. \\
&\quad \left. + \sum_{\ell < k} \left(\frac{1}{\phi^k} \eta^{k, \Lambda_k^{-1}(\ell)+1} \mathbb{I}(\ell \in \Lambda_k) - \sum_{t:k, \ell \in \Lambda_t} \frac{1}{\phi^t} \eta^{t, \Lambda_t^{-1}(k)+1} \eta^{t, \Lambda_t^{-1}(\ell)+1} \right) x_k x_\ell \right. \\
&\quad \left. + \sum_{k=1}^{n_x} \left(\frac{\eta^{k,1}}{\phi^k} - \sum_{\ell:k \in \Lambda_\ell} \frac{1}{\phi^\ell} \eta^{\ell,1} \eta^{\ell, \Lambda_\ell^{-1}(k)+1} \right) x^k \right\}, \tag{52}
\end{aligned}$$

where $\Lambda_\ell^{-1}(k)$ is the inverse function of $\Lambda_\ell(k)$, i.e. $\Lambda_\ell^{-1}(k) = t \Leftrightarrow \Lambda_\ell(t) = k$, and $\mathbb{I}(\ell \in \Lambda_k)$ is the indicator function returning one if $\ell \in \Lambda_k$ and zero otherwise. By setting equal corresponding coefficients in front of $(x^k)^2$, $x_k x_\ell$ and x_k in (51) and (52) we can identify the elements of μ and Q . Setting equal the coefficients in front of $(x^k)^2$ we get the diagonal elements of Q ,

$$Q^{k,k} = \frac{1}{\phi^k} + \sum_{\ell:k \in \Lambda_\ell} \frac{1}{\phi^\ell} \left(\eta^{\ell, \Lambda_\ell^{-1}(k)+1} \right)^2. \tag{53}$$

To get the non-diagonal elements we set equal the coefficients in front of $x_k x_\ell$. For $\ell < k$ we have

$$Q_{k,\ell} = Q_{\ell,k} = -\frac{1}{\phi^k} \eta^{k, \Lambda_k^{-1}(\ell)+1} \mathbb{I}(\ell \in \Lambda_k) + \sum_{t:k, \ell \in \Lambda_t} \frac{1}{\phi^t} \eta^{t, \Lambda_t^{-1}(k)+1} \eta^{t, \Lambda_t^{-1}(\ell)+1}. \tag{54}$$

In particular one should note that for $\ell < k$ we get $Q_{k,\ell} = 0$ if $\ell \notin \Lambda_k$ and there is no node t so that $k, \ell \in \Lambda_t$. This is what implies that Q is sparse. Finally, by equating corresponding coefficients in front of x_k we get

$$\sum_{\ell=1}^{n_x} \mu^\ell Q^{\ell,k} = \frac{\eta^{k,1}}{\phi^k} - \sum_{\ell:k \in \Lambda_\ell} \frac{1}{\phi^\ell} \eta^{\ell,1} \eta^{\ell, \Lambda_\ell^{-1}(k)+1}, \tag{55}$$

which can be used to find the elements of the mean vector μ . Since Q is sparse the strategy discussed in Section 2.1 can be used to compute μ efficiently.

B Derivation of posterior for hyperpriors

In the following we derive the posterior distribution for (η, ϕ) . In the derivation we simplify the notation by omitting the subscripts on the f 's as it should be clear from the context what densities we are dealing with. We start by identifying $f(\phi|x, z^{(m)})$ and thereafter find $f(\eta|\phi, x, z^{(m)})$.

Using the definitions of $f(x|\eta, \phi)$, $f(\phi)$ and $f(\eta|\phi)$ given in Section 4.1, and that $z^{(m)}$ and x are conditionally independent given ϕ and η , we get

$$\begin{aligned}
 f(\phi|z^{(m)}, x) &\propto f(\phi)f(z^{(m)}, x|\phi) \\
 &= f(\phi) \int f(\eta|\phi)f(z^{(m)}, x|\phi, \eta)d\eta \\
 &= f(\phi) \int f(\eta|\phi)f(x|\phi, \eta)f(z^{(m)}|\phi, \eta)d\eta \\
 &= f(\phi) \int f(\eta|\phi)f(x|\phi, \eta) \prod_{i \neq m} f(x^{(i)}|\phi, \eta)d\eta \\
 &= \prod_{k=1}^K \left[f(\phi^k) \int f(\eta^k|\phi^k)f(x^k|\phi^k, \eta^k, x^{\Lambda_k}) \prod_{i \neq m} f(x^{(i),k}|\phi^k, \eta^k, x^{\Lambda_k})d\eta^k \right] \\
 &\propto \prod_{k=1}^K f(\phi^k|z^{(m)}, x),
 \end{aligned}$$

where

$$\begin{aligned}
 f(\phi^k|z^{(m)}, x) &\propto f(\phi^k) \int f(\eta^k|\phi^k)f(x^k|\phi^k, \eta^k, x^{\Lambda_k}) \prod_{i \neq m} f(x^{(i),k}|\phi^k, \eta^k, x^{\Lambda_k})d\eta^k \\
 &= f(\phi^k) \cdot \frac{1}{(\phi^k)^{(|\Lambda_k|+\mathcal{M}+1)/2}} \int \exp \left\{ -\frac{1}{2}(\eta^k - \zeta^k)^T (\phi^k \Sigma_{\eta^k})^{-1} (\eta^k - \zeta^k) \right. \\
 &\quad \left. - \frac{1}{2\phi^k} (x^k - (1, (x^{\Lambda_k})^T) \eta^k)^2 - \frac{1}{2\phi^k} \sum_{i \neq m} (x^{(i),k} - (1, (x^{(i), \Lambda_k})^T) \eta^k)^2 \right\} d\eta^k.
 \end{aligned} \tag{56}$$

We note that the exponent in the integrand is a second order function in η^k , so by completing the square it is straightforward to evaluate the integral analytically. When having evaluated the integral and inserting for $f(\phi^k)$ this gives, using the notation defined in (38) to (40),

$$\begin{aligned}
 f(\phi^k|z^{(m)}, x) &\propto \frac{e^{-\frac{1}{\phi^k \beta^k}}}{(\phi^k)^{\alpha^k+1}} \cdot \frac{1}{(\phi^k)^{\mathcal{M}/2}} e^{-\frac{1}{2\phi^k} (\gamma^{m,k} - (\rho^{m,k})^T (\Theta^{m,k})^{-1} \rho^{m,k})} \\
 &= \frac{e^{-\frac{1}{\phi^k \beta^{m,k}}}}{(\phi^k)^{\bar{\alpha}^k+1}},
 \end{aligned}$$

where $\tilde{\alpha}^k$ and $\tilde{\beta}^{m,k}$ are as given in (36) and (37), respectively. We recognise this as the density of a inverse gamma distribution, so

$$\phi^k | z^{(m)}, x \sim \text{InvGam}(\tilde{\alpha}^k, \tilde{\beta}^{m,k}). \quad (57)$$

This concludes the derivation of the posterior distribution for ϕ , and we proceed to the derivation of the posterior for $\eta | \phi$. Using the definitions of $f(x | \eta, \phi)$ and $f(\eta | \phi)$ we get

$$\begin{aligned} f(\eta | x, z^{(m)}, \phi) &\propto f(\eta | \phi) f(x, z^{(m)} | \eta, \phi) = f(\eta | \phi) f(x | \eta, \phi) \prod_{i \neq m} f(x^{(i,m)} | \eta, \phi) \\ &= \prod_{k=1}^K \left[f(\eta^k | \phi^k) f(x^k | \eta^k, \phi^k, x^{\Lambda_k}) \prod_{i \neq m} f(x^{(i),k} | \eta^k, \phi^k, x^{\Lambda_k}) \right] \\ &\propto \prod_{i \neq m} f(\eta^k | x, z^{(m)}, \phi^k), \end{aligned}$$

where

$$\begin{aligned} f(\eta^k | x, z^{(m)}, \phi^k) &\propto f(\eta^k | \phi^k) f(x^k | \eta^k, \phi^k, x^{\Lambda_k}) \prod_{i \neq m} f(x^{(i),k} | \eta^k, \phi^k, x^{\Lambda_k}) \\ &\propto \frac{1}{(\phi^k)^{(|\Lambda_k| + \mathcal{M} + 1)/2}} \exp \left\{ -\frac{1}{2} (\eta^k - \zeta^k)^T (\phi^k \Sigma_{\eta^k})^{-1} (\eta^k - \zeta^k) \right\} \\ &\times \exp \left\{ -\frac{1}{2\phi^k} (x^k - (1, (x^{\Lambda_k})^T) \eta^k)^2 - \frac{1}{2\phi^k} \sum_{i \neq m} (x^{(i),k} - (1, (x^{(i),\Lambda_k})^T) \eta^k)^2 \right\}. \end{aligned}$$

Again introducing $\gamma^{i,k}$, $\rho^{i,k}$ and $\Theta^{i,k}$, as defined in (38) to (40) this can be simplified to

$$f(\eta^k | x, z^{(m)}, \phi^k) \propto \exp \left\{ -\frac{1}{2\phi^k} (\eta^k - (\Theta^{m,k})^{-1} \rho^{m,k})^T \Theta^{m,k} (\eta^k - (\Theta^{m,k})^{-1} \rho^{m,k}) \right\},$$

which we recognise as the density of a normal distribution, so

$$\eta^k | x, z^{(m)}, \phi^k \sim N((\Theta^{m,k})^{-1} \rho^{m,k}, \phi^k (\Theta^{m,k})^{-1}). \quad (58)$$

Thereby the derivation of $f(\eta, \phi | x, z^{(m)})$ is complete.

References

Bocquet M (2011) Ensemble kalman filtering without the intrinsic need for inflation. *Nonlinear Processes in Geophysics* **18**:735–750

- Bocquet M, Raanes PN, Hannart A (2015) Expanding the validity of the ensemble Kalman filter without the intrinsic need for inflation. *Nonlinear Processes in Geophysics* **22**:645–662
- Brockwell PJ, Davis RA (1990) *Time Series: Theory and Methods*, 2nd edn. Springer
- Burgers G, van Leeuwen PJ, Evensen G (1998) Analysis scheme in the ensemble Kalman filter. *Monthly Weather Review* **126**:1719–1724
- Chan JCC, Strachan RW (2020) Bayesian state space models in macro-econometrics. *Journal of Economic Surveys* To appear
- Creal D (2011) A survey of sequential Monte Carlo methods for economics and finance. *Econometric Reviews* **31**:245–296
- Cressie N, Davidson J (1998) Image analysis with partially ordered Markov models. *Computational Statistics and Data Analysis* **29**:1–26
- Doucet A, Johansen AM (2011) A tutorial on particle filtering and smoothing: Fifteen years later. *Oxford Handbook of Nonlinear Filtering* **12**
- Doucet A, de Freitas N, Gordon N (2001) *Sequential Monte Carlo Methods in Practice*. Springer Verlag, New York
- Evensen G (1994) Sequential data assimilation with a nonlinear quasi-geostrophic model using monte carlo methods to forecast error statistics. *Journal of Geophysical research* **99**:10,143–10,162
- Evensen G (2009) *Data Assimilation. The Ensemble Kalman Filter*, 2nd edn. Springer, Dordrecht
- Haugen VEJ, Evensen G (2002) Assimilation of sla and sst data into an ogcm for the indian ocean. *Ocean Dynamics* **52**:133–151
- Hotta D, Ota Y (2021) Why does EnKF suffer from analysis overconfidence? an insight into exploiting the ever-increasing volume of observations. *Quarterly Journal of the Royal Meteorological Society* **147**:1258–1277
- Houtekamer PL, Mitchell HL (1997) Data assimilation using an ensemble Kalman filter technique. *Monthly Weather Review* **126**:796–811
- Houtekamer PL, Zhang F (2016) Review of the ensemble kalman filter for atmospheric data assimilation. *Monthly Weather Review* **144**:4489–4532
- Janjic T, Nerger L, Albertella A, et al (2011) On domain localization in ensemble-based kalman filter algorithms. *Monthly Weather Review* **139**:2046–2060

- Kalman R (1960) A new approach to linear filtering and prediction problems. *Journal of Basic Engineering, Transactions of the ASME* **82**:35–46
- Kalman R, Bucy R (1961) New results in linear filtering and prediction theory. *Journal of Basic Engineering, Transactions of the ASME* **83**:95–108
- Katzfuss M, Stroud JR, Wikle CK (2016) Understanding the ensemble kalman filter. *The American Statistician* **70**:350–357
- Katzfuss M, Stroud JR, Wikle CK (2020) Ensemble Kalman methods for high-dimensional hierarchical dynamic space-state models. *Journal of American Statistical Association* **115**:866–885
- Loe MK, Tjelmeland H (2020) Ensemble updating of binary state vectors by maximizing the expected number of unchanged components. *Scandinavian Journal of Statistics* **48**:1148–1185
- Loe MK, Tjelmeland H (2021) A generalised and fully bayesian framework for ensemble updating. Tech. rep., ArXiv e-prints 2103.14565, Available from <https://doi.org/10.48550/arXiv.2103.14565>
- Loe MK, Tjelmeland H (2022) Ensemble updating of categorical state vectors. *Computational Statistics*
- Loeliger HA, Dauwels J, Hu J, et al (2007) The factor graph approach to model-based signal processing. *Proceedings of the IEEE* **95**:1295–1322
- Luo X, Hoteit I (1997) Covariance inflation in the ensemble Kalman filter: A residual nudging perspective and some implications. *Monthly Weather Review* **126**:796–811
- Myrseth I, Sætrom J, Omre H (2013) Resampling the ensemble Kalman filter. *Computers and Geosciences* **55**:44–53
- Omre H, Myrseth I (2010) Hierarchical ensemble kalman filter. *SPE Journal* **15**:569–580
- Rue H, Held L (2005) *Gaussian Markov Random Fields*. Chapman & Hall/CRC
- Shumway RH, Stoffer DS (2016) *Time Series Analysis and Its Applications*, 4th edn. Springer
- Smith AC, Emery N (2003) Estimating a state-space model from point process observations. *Neural Computation* **15**:965–991
- Sætrom J, Omre H (2013) Uncertainty quantification in the ensemble kalman filter. *Scandinavian Journal of Statistics* **40**:868–885

Tsyrlunikov M, Rakitko A (2017) A hierarchical Bayes ensemble Kalman filter. *Physica D* **338**:1–16

Woodbury MA (1950) Inverting modified matrices. Memorandum report 42, Statistical Research group, Princeton University, Princeton, NJ